

## A FUZZY-SMC-PI LOAD FREQUENCY CONTROL FOR MODERN POWER SYSTEMS WITH RENEWABLE ENERGY SOURCES

SAMIR E. ESHO and LOKMAN H. HASSAN

Dept. of Electrical and Computer Engineering, College of Engineering, University of Duhok, Kurdistan Region-Iraq

*(Received: September 5, 2024; Accepted for Publication: October 13, 2024)*

### ABSTRACT

In this paper, a Fuzzy Sliding Mode and PI (Fuzzy-SMC-PI) controller is presented for the Load Frequency Control (LFC) of hybrid power systems. The fuzzy controller acts as a supervisory controller for the sliding mode control and the conventional PI control. The proposed LFC overcomes the problems of overshoot and slow transient responses of the PI controller in the transient state and the chattering problem related to the robust sliding mode controller in the steady state. The controller is applied to a three-area hybrid power system made up of conventional thermal, solar thermal, and an Electric Vehicle (EV). The results showed lower noise, overshoot and a significant reduction of settling time when compared to existing approaches.

**KEYWORDS:** Load Frequency Control (LFC), Fuzzy Logic (FL), PI controller, Sliding Mode Control (SMC).

### 1. INTRODUCTION

Load Frequency Control (LFC) is a crucial function in power systems that ensures system frequency and tie-line power exchange remain within acceptable limits. By dynamically balancing power generation with load demand, LFC maintains frequency stability. Traditional LFC methods, relying on Proportional-Integral (PI) controllers, have become increasingly inadequate with the integration of Renewable Energy Sources (RES). The intermittent nature and reduced inertia of RES introduce complexities that PI controllers struggle to handle. This has led to a search for more robust and effective LFC strategies (Ahmad, Zhang, & Yan, 2020).

Various control techniques have been proposed, including classical approaches, soft computing, and Artificial Intelligence (AI) methods. Classical techniques like Proportional-Integral-Derivative (PID) control have limitations in handling modern power grid complexities. Adaptive control and optimal control techniques have been explored to address these limitations. AI techniques, such as Fuzzy Logic (FL), Artificial Neural Networks (ANNs), Genetic Algorithms (GA), and Particle Swarm Optimization (PSO), offer potential solutions for the challenges posed by RES integration (Aditya, 2010; Kang, Wang, & Wu, 2006; Kumar, 1998;

Nikzad et al., 2010; Rerkpreedapong, Hasanovic, & Feliachi, 2003; Sabahi, Sharifi, Aliyari-Shoorehdeli, M, & Aliasghary, 2008).

Fuzzy logic, with its ability to handle uncertainty and imprecision, has shown promise in mitigating oscillations and ensuring smooth operation (Anand & Jeyakumar, 2008; Aravindan & Sanavullah, 2011). Sliding Mode Control (SMC), known for its robustness and fast response time, has also emerged as a promising technique (Yang et al., 2014). However, both fuzzy control and SMC have limitations, such as the need for expert knowledge and the potential for chattering.

Fuzzy Logic Control (FLC) has emerged as a promising solution for LFC in power systems, demonstrating superior performance in addressing these challenges. In (Mohamed, Hassan, Moghavvemi, & Yang, 2008) and (Hassan, Mohamed, Moghavvemi, & Yang, 2009), a Fuzzy Gain Scheduled Proportional and Integral (FGPI) and Fuzzy Gain Scheduled Integral and Derivative (FGID) controllers introduced for LFC of a multi-area system including two hydropower plants and a two-area hydropower system respectively. The developed controller showed better results when compared to conventional controllers. In addition, FGID showed better performance than a PID-based GA controller. Khooban, M. H., and Niknam, T. (Khooban & Niknam, 2015) proposed a LFC for

a four-area power system using a combination of self-adaptive modified bat algorithm and FL. The method was conducted to optimize PI controller parameters and FL membership functions, aiming to achieve stability, robustness, and optimal performance against external disturbances and dynamic changes. Zahid Farooq et al. (Farooq, Rahman, & Lone, 2021) developed a FLC to optimize the gains of optimal Integral Double Derivative IDD controller-based LFC of a three-area multi-sources electrical power system. The used controller aims to optimize performance and quickly restore frequency after load variation. Diem-Vuong Doan et al. (Doan, Nguyen, & Thai, 2021) proposes a new PID-based fuzzy logic controller for a two-area interconnected power system with RES to achieve better dynamic performance (i.e. smallest overshoots and settling times) during a load disturbance. A Fuzzy Rule-tuned PID (FRT-PID) controller optimized by the Coronavirus Herd immunity optimizer algorithm was proposed by Jyotirmoy Biswas et al. (Biswas, Bera, & Chakrabarty, 2023) for LFC within each control area. The effectiveness of the FRT-PID controllers was evaluated through comparisons with conventional PID controllers under various load disturbances, demonstrating improved LFC performance. The application of a FLC for automatic generation control and automatic voltage regulation in a four-area interconnected hydropower facility was investigated by Abdulkerim Ali et al. (Ali, Biru, & Banteyirga, 2023). The objective was to improve frequency and voltage regulation compared to traditional PI and PID controllers under varying load conditions.

SMC offers a robust control approach for LFC by forcing the system to a pre-defined switching surface. This ensures fast transient response and high tracking accuracy, making it attractive for LFC applications. However, SMC can introduce chattering, a high-frequency oscillation around the switching surface, which can led to increased control effort and stress on system components. K. Vrdoljak et al. (Vrdoljak, Peric, & Petrovic, 2010) proposed a novel Discrete-time Sliding Mode Controller (DSMC) with state estimation for LFC in power systems. Unlike traditional controllers, the DSMC with full-state feedback via fast-sampled measurements is applicable to both thermal and hydro plants. A genetic algorithm optimizes the DSMC design, leading to superior performance compared to PI controllers. To address frequency deviations caused by wind power in interconnected systems, Yang Mi et al.

(Mi et al., 2014) explored a new LFC approach using a decentralized SMC technique for multi-area power systems, including wind turbines. The SMC design precisely tackles uncertainties caused by governors, variable turbine operation, and wind power fluctuations. R. Mondai and M. M. Rahman (Mondai & Rahman, 2017) proposed a variable structure concept of sliding mode-based LFC on a two-area interconnected power system to regulate the frequency error, tie-line power error and area control error despite the presence of external load disturbance and system uncertainties. Yiwen Xu (Xu et al., 2020) developed an adaptive sliding mode LFC with a super-capacitor and battery energy storage system for an interconnected power system with wind power to study frequency deviation caused by RES. An Integral Sliding Mode Control with Neural Networks (I-SMC-NN) control strategy was proposed in (Qian, Tong, Liu, & Liu, 2016) for LFC in power systems with wind and Generation Rate Constraint (GRC) constraints. NNs handle uncertainties from wind and linearized GRC, and Lyapunov-based weight updates ensure stability. Zhiwen Deng et al. (Deng, Xu, Huo, Han, & Xue, 2022) proposed an Adaptive Fuzzy Super-Twisting Sliding Mode Control (AF-SSMC) method to maintain power grid stability with increasing wind power integration. The system uses battery storage to smooth out wind power fluctuations and improve the grid's ability to handle changes in demand LFC. A novel control method, State Observer based on Sliding Mode Control (SOboSMC), for regulating frequency and tie-line power flow in multi-area interconnected power systems was introduced by Huynh, V.V. et al. (Huynh, Minh, Amaefule, Tran, & Tran, 2021). SOboSMC addresses the challenges of modern power plants, including load disturbances, uncertainties, and parameter measurement difficulties, especially in systems with integrated wind farms. Asghar, R. et al. (Asghar, Riganti Fulginei, Wadood, & Saeed, 2023) provided a comprehensive review of LFC advancements in wind-powered systems. It analyzes diverse control strategies, including classical, AI-based and novel approaches like sliding mode and cascade control.

While both Fuzzy and SMC offer advantages for LFC in modern power systems with RES, they come with some challenges. Fuzzy control despite its flexibility and robustness, requires significant expertise and time investment to fine-tune its membership functions and control rules. Additionally, analyzing stability within a fuzzy

control framework can be mathematically complex. On the other hand, SMC offers a fast response but it can introduce a phenomenon called "chattering" which leads to increased wear and tear on system components and higher power losses. Designing robust SMC controllers for complex systems with uncertainties like those found with RES integration can also be difficult.

To address the advantages and the limitations of PI, fuzzy and SMC control techniques, the proposed research introduces a novel Fuzzy-SMC-PI control strategy for LFC in modern power systems with RES. The proposed hybrid approach merges the strengths of each method to achieve a robust and adaptable solution. FL provides a high-level adaptable decision layer that simplifies tuning the SMC and PI components. SMC ensures fast response and high tracking accuracy overcoming potential sluggishness in pure fuzzy control. Finally, a PI controller tackles steady-state errors and improves overall system performance. By combining these elements, the Fuzzy-SMC-PI controller has the potential to effectively manage LFC in modern power systems with RES integration. The primary aim is to demonstrate its effectiveness in maintaining frequency stability and overcoming the challenges posed by RES integration. This translates to developing a fast and adaptable controller capable of reducing overshoots, settling time and mitigating the impact of load disturbances. Ultimately, the proposed research strives to contribute to the reliable and stable operation of RES-integrated power grids. Further, the proposed controller is compared with a fuzzy-optimized IDD controller (Farooq et al., 2021) and conventional controllers which are also simulated in this paper under different scenarios to show its robust performance.

The rest of the paper is organized as; section 2 clarifies the used model of an unequal three area hybrid power system incorporating EV. Section 3 give the details about the design of the proposed controller. Section 4 shows the results and discussion of the proposed fuzzy SMC-PI controller to assess the effectiveness of the proposed approach when it is compared with fuzzy-optimized IDD controller and conventional controllers under different operating conditions. Finally, Section 5 concludes the paper by

summarizing the key findings and potential implications of the research.

## 2. MODELING OF A POWER SYSTEM WITH RENEWABLE ENERGY SOURCES

The transfer function model of a three-area hybrid power system for LFC incorporating EVs accurately represents a modern power system with diverse energy sources, including conventional-thermal, solar-thermal, and EV with the utility grid (Farooq et al., 2021). The model captures key features such as the presence of EVs in area 1 and area 2, time delays in each area, GRC limitations of conventional thermal plants, time delays in solar thermal plants, and the ability of EVs to charge from or discharge to the grid. The model is calibrated using nominal system values for conventional thermal, solar thermal, and EVs from (Gaur, Bhowmik, & Soren, 2019; Kothari, Singapore, 2003.; Saha & Saikia, 2018; Tasnin & Saikia, 2017). MATLAB Simulink program and MATLAB Fuzzy Logic Toolbox provide a robust platform for modeling, designing of the controller, simulating, and analyzing the dynamic behavior of power systems. All system parameters are given in Appendix A.

The three-area power system, with a 2:3:4 capacity ratio, was designed to study LFC under various conditions. Area-1 and area-2 included conventional-thermal, solar-thermal, and EV components, while Area-3 comprised conventional-thermal and EV. Each control area had a time delay of 0.2 seconds, conventional thermal plants had a GRC of 3% per minute, and solar thermal plants had a 0.5-second time delay.

Under nominal conditions, the system operates at 50% loading, with 1% SLP in area-1 and uniform solar irradiance of 800 W/m<sup>2</sup>. From the block diagram model, it is clearly seen that there are three control inputs named u<sub>1</sub>, u<sub>2</sub> and u<sub>3</sub>. The block diagram shown in Fig. (1), which represents a three-area power system model with three control areas connected to each other through a line having its own dynamics called tie line.

### 2.1 Modelling of the Multi-Area Power System

#### 2.1.1. Modelling of the Thermal Power System

The transfer functions of the thermal power system that is consist of a generator, governor, turbine and reheater are described as:

T.F of the governor is:

$$G_{gi}(s) = \frac{1}{1+s T_{gi}} \quad (1)$$

where  $T_{gi}$  is the steam governor time constant for the thermal power plant of area i, sec.

T.F of the reheater is:

$$G_{ri}(s) = \frac{1 + s K_{ri} T_{ri}}{1 + s T_{ri}} \quad (2)$$

where  $K_{ri}$  and  $T_{ri}$  are the reheat turbine gain and reheat turbine time constant for the thermal power plant of area i.

T.F of the turbine is:

$$G_{ti}(s) = \frac{1}{1 + s T_{ti}} \quad (3)$$

where  $T_{ti}$  is the time constant of the turbine of area i, sec.

T.F of the thermal generator is:

$$G_{Pi}(s) = \frac{K_{Pi}}{1 + s T_{Pi}} \quad (4)$$

where,  $K_{Pi}$  is the power system gain for area i and equal to  $\frac{1}{D_i}$ ,  $D_i$  is the system damping coefficient of area i and  $T_{Pi}$  is the power system time constant of area i.

### 2.1.2. Modelling of the photovoltaic system

The transfer function of the solar photovoltaic system including PV panel, maximum power point tracker, converter and filter is given by:

$$G_{PV}(s) = \frac{K_{DSTS}}{1+s T_{DSTS}} \quad (5)$$

where  $K_{DSTS}$  and  $T_{DSTS}$  are the gain and the time constant of the solar thermal system.

### 2.1.3. Modelling of the Electric Vehicles

The transfer function of the electric vehicles system is given by:

$$G_{EV}(s) = \frac{K_{EV}}{1+s T_{EV}} \quad (6)$$

where  $K_{EV}$  and  $T_{EV}$  are gain and time constant of the electrical vehicle.



### 3. FUZZY SMC-PI CONTROLLER

The combined fuzzy-SMC-PI controller is designed for LFC as shown in Fig. 2. The new controller improves power systems frequency and it merges three powerful techniques:

- **Sliding Mode Control (SMC):** SMC ensures the system rapidly reaches a desired operating point. It establishes a "sliding surface" representing the ideal system trajectory. The controller steers the system towards this surface using a control signal that hinges on the system's distance from it.
- **Proportional-Integral Control (PI Control):** PI control excels in steady-state performance by eliminating any residual error after reaching the sliding surface. The proportional term reacts to the current error, while the integral term eliminates long-term bias.
- **Fuzzy Logic Control (FLC):** Unlike conventional control methods, FLC leverages human-like reasoning with linguistic terms ("high" or "low"). These features empower FLC

to adapt to non-linearities and uncertainties inherent in power grids. Automatic Control Error (ACE) and its rate of change (ACE) as selected to be inputs for the FLC. FLC will act as a supervisory controller for the sliding mode control and the conventional PI control based on its output gains values (i.e.  $K_I$  and  $K_S$ ). The fuzzy-SMC-PI controller revolutionizes LFC in power systems by merging the strengths of three powerful techniques. Fuzzy logic's adaptability, achieved through membership functions, tackles non-linearities and uncertainties in power grids. Sliding mode control ensures a rapid response to load changes by driving the system towards a stable frequency. This synergistic effect is further enhanced by PI control, which minimizes frequency deviations and settling times for smoother power delivery by continuously adjusting the output based on both the current error and its rate of change. As a result, exceptional robustness against parameter variations within the power grid is achieved.

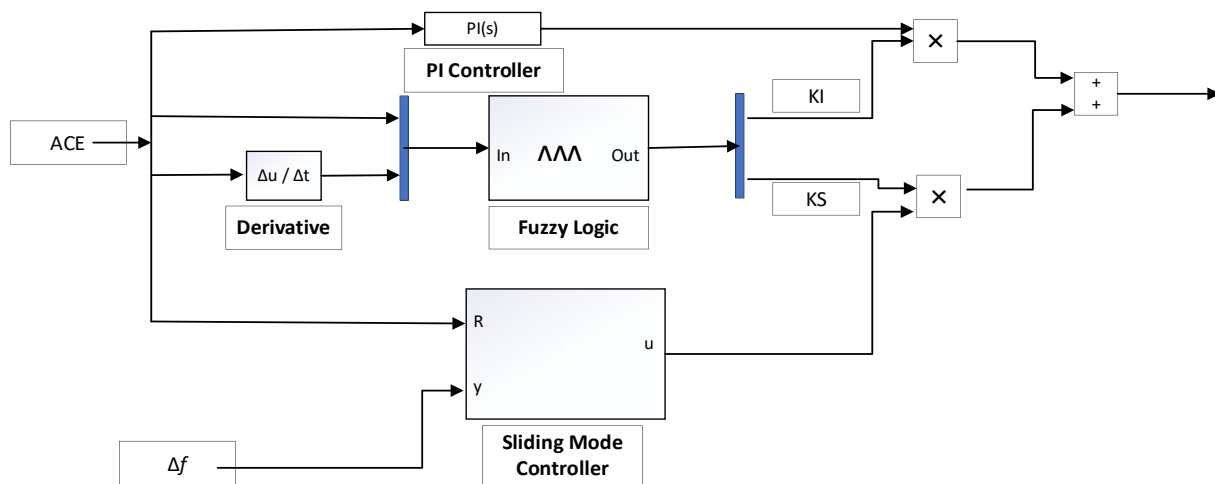


Fig. (2): Block diagram of Fuzzy-SMC-PI controller.

The process of the used control is explained in the following points:

1. **Error Measurement:** The system continuously monitors the frequency and calculates  $(\Delta f)$  and  $(\dot{\Delta f})$ .
2. **Fuzzification:** FLC translates the crisp values of error and its derivative (i.e. ACE and ACE) into membership degrees for predefined fuzzy sets.
3. **Rule Evaluation:** Based on the membership degrees, FLC activates relevant fuzzy rules that define adjustments for  $K_S$  and  $K_I$ .
4. **Defuzzification:** The activated rules' consequences are aggregated to obtain crisp values for  $K_S$  and  $K_I$ .

5. **PI Controller Update:** The PI controller's gains are adjusted by  $K_I$ , influencing its response to the frequency error.

6. **Sliding Mode Control:** The output of the SMC is adjusted by  $K_S$ , showing its response to the frequency error.

The proposed FLC is Sugeno-type. The intervals for error and its derivative are normalized to be within range  $[0,1]$ . To enhance its effectiveness, seven linguistic variables are employed for the inference mechanisms i.e., negative large (NL), positive large (PL), negative medium (NM), positive medium (PM), negative small (NS), positive small (PS), and zero (ZR). For simplicity, triangular membership functions

are employed for the two inputs, ACE and  $\dot{ACE}$ , as shown in Fig. 3. A set of fuzzy rules is established to optimize the controller gains based on the values of ACE and its change. This rule base is presented in Table 1.

Human expertise and system response analysis are used to build fuzzy rules for tuning the integral ( $K_I$ ) and sliding mode ( $K_S$ ) parameters.

A large error means a big difference from the target and the state is far from the set-point and will take time to reach it. To speed up the process, a strong control action is needed to achieving the target. This is achieved by increasing the sliding mode gain. However, a small error means the response is close to the target and the state is near to the steady state area. Here, a small sliding mode gain is best to avoid overshoot, while a large integral gain helps to reach the target value quickly.

On the other hand, the change in the error indicates the rate at which the state is changing. A small change needs a large sliding mode gain for large errors, but a large change needs a large

sliding mode gain for large errors and moderate integral gain for small errors. Fig. 4 shows the fuzzy tuning rules, and Table 1 provides a simpler way to understand them.

In LFC loop, Area Control Error (ACE) includes change in tie-line power,  $\Delta P_{tie}$  and change in frequency,  $\Delta f$  given to the controller as input. ACE is a signal that reflects the deviation between the actual and desired operating conditions in a specific control area of the power system. It considers both frequency and net interchange power (i.e. the difference between power exported and imported by the area) as shown in Fig. 2. The input ACE in LFC loop for a particular area  $i$  is given by equation (7).

$$ACE_i = \Delta P_{tie\ i} + B_i \times \Delta f_i \quad (7)$$

where:

- $\Delta P_{tie\ i}$ : Deviation in net interchange power for area  $i$  (actual - scheduled)
- $B_i$ : Frequency bias constant of area  $i$  (a weighting factor)
- $\Delta f_i$ : Deviation in frequency for area  $i$  (actual - scheduled)

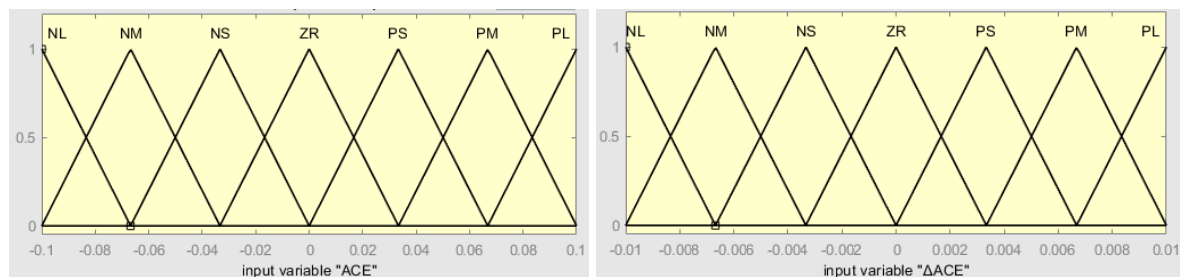


Fig. (3): Membership functions of ACE and  $\dot{ACE}$

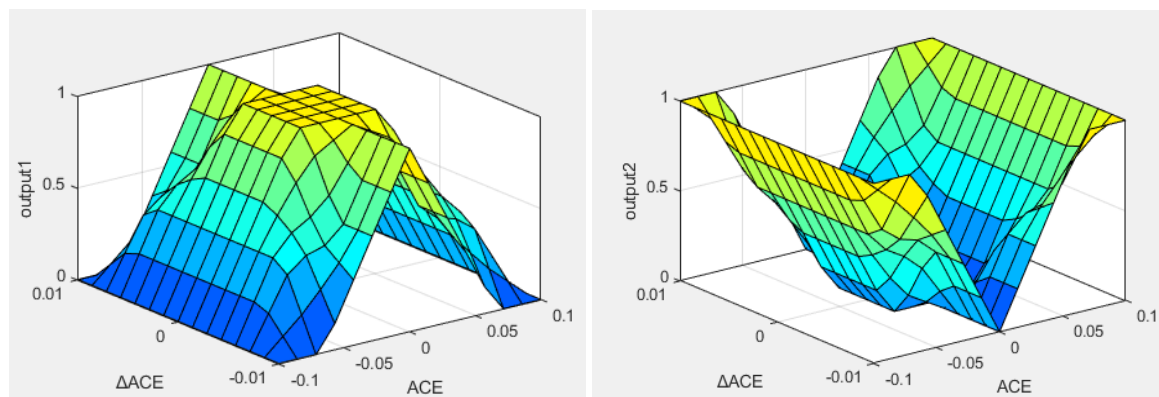


Fig. (4): Three-dimensional plot for rule base of  $K_I$  and  $K_S$ .

**Table (1):** Fuzzy logic rules for  $K_I$  and  $K_S$ .

ACE / ACE	NL	NM	NS	ZR	PS	PM	PL
NL	Z, B	Z, B	Z, B	Z, B	Z, B	Z, B	Z, B
NM	Z, B	M, M	M, M	M, M	M, M	M, M	Z, B
NS	M, M	M, M	B, Z	B, Z	B, Z	M, M	M, M
ZR	B, Z	B, Z	B, Z	B, Z	B, Z	B, Z	B, Z
PS	M, M	M, M	B, Z	B, Z	B, Z	M, M	M, M
PM	Z, B	M, M	M, M	M, M	M, M	M, M	Z, B
PL	Z, B	Z, B	Z, B	Z, B	Z, B	Z, B	Z, B

The outputs of the fuzzy rules are categorized into Big (B), Moderate (M), and Zero (Z) levels as singleton spikes. For instance, when the error is significantly negative (NL) and the change is negligible (ZR), a large slide mode gain (B) is needed for a strong corrective action. However, a small integral gain (Z) avoids overshoot.

Therefore, the rule representing this case can be written as:

If ACE is NL and ACE is ZR then  $K_S$  is B and  $K_I$  is Z

At the point with ACE is NS and ACE is PS, only a large integral gain will eliminate any remaining error. The rule can then be written as:

$$WA = \frac{\mu(c_1) \times c_1 + \mu(c_2) \times c_2 + \dots + \mu(c_i) \times c_i}{\mu(c_1) + \mu(c_2) + \dots + \mu(c_i)} \tag{8}$$

where i is a number of singleton spikes.

By applying these rules, the fuzzy-SMC-PI controller gains are automatically adjusted. An important aspect of the proposed design is that the fuzzy-SMC-PI controller is implemented in all areas of the hybrid power system. While the rule base remains the same, the membership ranges for controller gains are customized for each area. This allows each area to independently determine the optimal controller gains. This customization is crucial in multi-area power systems to minimize unintended power exchange during frequency fluctuations.

#### 4. RESULTS AND DISCUSSION

The proposed Fuzzy-SMC-PI controller's performance was rigorously assessed in a simulated three-area hybrid power system. The system consists of conventional thermal plants, solar-thermal energy and electric vehicles reflecting a modern grid with renewable integration. The system with the proposed

If ACE is NS and ACE is PS then  $K_S$  is Z and  $K_I$  is B

When ACE is PM and ACE is NM, a moderate slide mode gain (M) provides a balanced response. A moderate integral gain (M) helps settle the error without causing overshoot. The rule can then be written as:

If ACE is PM and ACE is NM then  $K_S$  is M and  $K_I$  is M

In the defuzzification process, the Weight Average (WA) method is used:

controller is implemented within the MATLAB Simulink environment. The controller's effectiveness was evaluated under various Step Load Perturbation (SLP). To gauge the proposed controller superiority, comparisons were carried out against a Fuzzy-IDD controller, I, PI and PID load frequency controllers. The performance of each controller will be assessed by examining the dynamic responses of the system in terms of Maximum Overshoot (MO), Maximum Undershoot (MU), and Settling Time (TS). This evaluation aimed to demonstrate the Fuzzy-SMC-PI controller's ability to maintain system frequency within acceptable limits and regulate tie-line power exchange during frequency fluctuations, ultimately achieving superior load frequency control in complex power systems with renewable energy sources.

The system with the fuzzy-SMC-PI controllers is tested under nominal conditions with the system operating at 50% of its rated load. The receiving solar irradiance is 800 W/m<sup>2</sup>. The

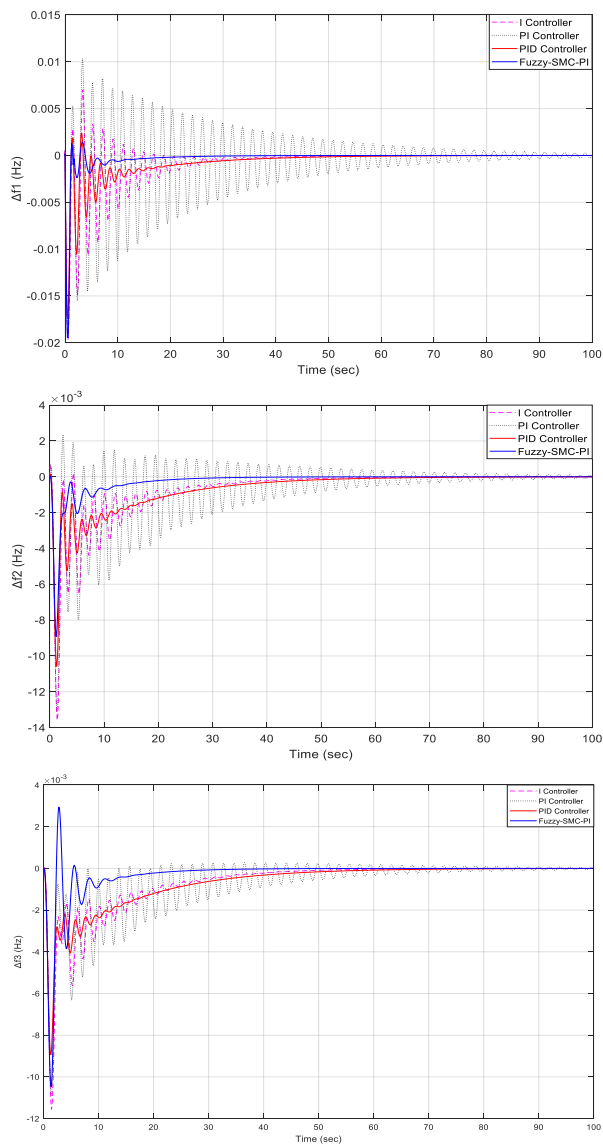
time delay of each control area is 0.2 sec. GRC of 3% per minute is considered for each conventional-thermal plant. Here, the system is subjected to different SLP percentage at different areas creating three scenarios.

#### 4.1 The System Response of Scenario 1

The system with the fuzzy-SMC-PI controllers is subjected to a 1% SLP in area-1. The system dynamic responses are shown in Fig. 5.

The proposed controller performances are compared against an I, PI and PID load frequency

controllers. The comparison of the controller performances revealed that the Fuzzy-SMC-PI controller exhibited the most favorable characteristics (see Table 2). The Fuzzy-SMC-PI controller's responses were non-oscillatory, with minimal settling time, undershoots and relatively smaller overshoots. This superior performance of the Fuzzy-SMC-PI controller can be attributed to its ability to effectively handle the inherent complexities of the hybrid power system which incorporates both conventional thermal power generation and renewable energy sources.



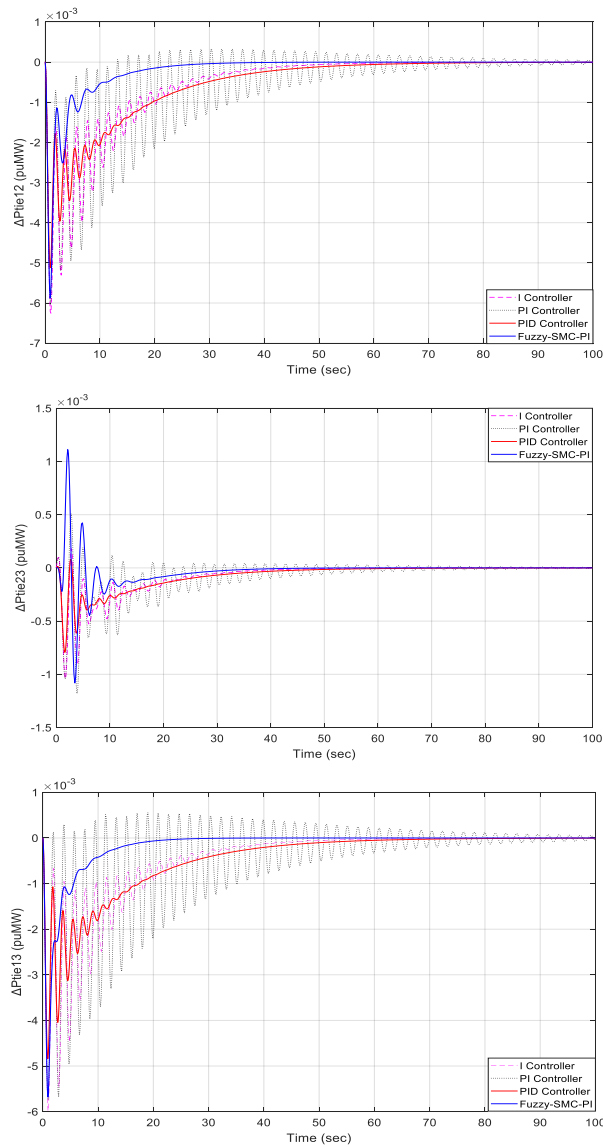


Fig. (5): The system response with I, PI, PID & Fuzzy-SMC-PI controllers

Table (2): The system response with I, PI, PID and Fuzzy-SMC-PI controllers

	I Controller			PI Controller			PID Controller			Fuzzy-SMC-PI Controller		
	MO	MU	TS	MO	MO	TS	MO	MU	TS	MO	MU	TS
$\Delta f_1$	0.007	-0.019	35	0.01	-0.019	94	0.0024	<b>-0.017</b>	37	<b>0.0014</b>	-0.019	<b>13</b>
$\Delta f_2$	0.0007	-0.013	38	0.0023	-0.013	79	0.0001	-0.01	45	-	<b>-0.0089</b>	<b>21</b>
$\Delta f_3$	-	-0.011	39	-	-0.011	70	-	-0.011	48	0.0029	<b>-0.010</b>	<b>20</b>
$\Delta P_{tie12}$	-	-0.0062	41	0.0003	-0.006	87	-	-	51	-	-0.0058	<b>21</b>
								<b>0.0052</b>				
$\Delta P_{tie23}$	0.0002	-0.001	38	0.0005	-0.0011	76	-	-	48	0.0011	-0.001	<b>32</b>
								<b>0.0008</b>				
$\Delta P_{tie13}$	-	-0.006	41	0.0005	-0.0057	97	-	-	50	-	<b>-0.0056</b>	<b>17</b>
								0.0058				

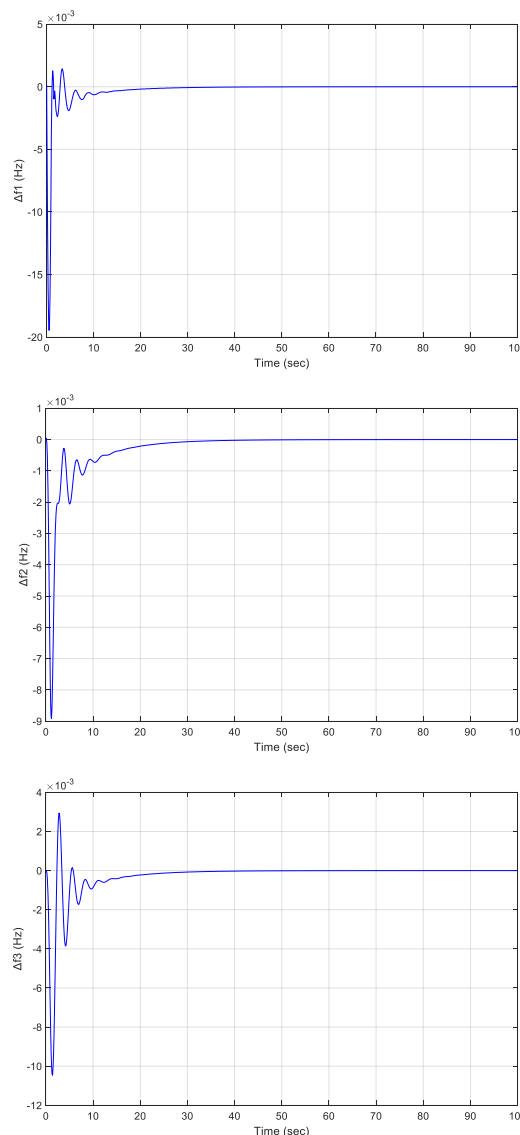
Note: Bold values indicate dominating values

Also, the proposed controller performances are compared with a fuzzy optimized IDD controller (Farooq et al., 2021).

The system dynamic responses for the fuzzy-SMC-PI controller are shown in Fig. 6 and the results reported in Table 3. Data provided in Table 3 gives the comparative performance analysis of both the controllers. The results show that the fuzzy-SMC-PI controller outperforms the fuzzy optimized IDD controller. To further compare the two controllers, a Demerit Index (DI) was calculated. DI is a measure of the controller's performance and a lower DI value

indicates better performance. The DI values for both controllers are reported in Table 4 using equation (9). The critical review of these values clearly highlights the dominance of fuzzy-SMC-PI controller performance in terms of MO, TS and DI. The critical analysis of the DI values for each of the system dynamic responses verifies supremacy of the fuzzy-SMC-PI controller over the fuzzy-IDD controller.

$$DI = (MO)^2 + (MU)^2 + (TS)^2 \tag{9}$$



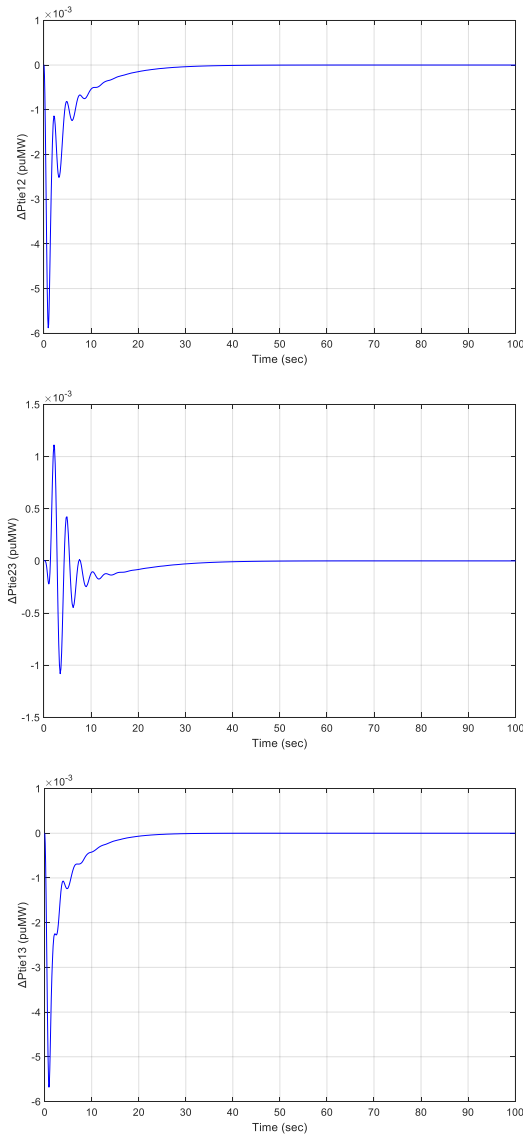


**Fig. (6):** The system response with Fuzzy-SMC-PI controller at 1% SLP in area-1

**Table (3):** The system response with Fuzzy-IDD and Fuzzy-SMC-PI controllers

	Fuzzy IDD Controller			Fuzzy SMC-PI Controller		
	MO	MU	TS	MO	MU	TS
$\Delta f_1$	<b>0.0002</b>	-0.028	13.21	0.0014	<b>-0.019</b>	<b>13.07</b>
$\Delta f_2$	-	-0.027	24.61	-	<b>-0.0089</b>	<b>21</b>
$\Delta f_3$	-	-0.021	24.25	0.0029	<b>-0.010</b>	<b>20</b>
$\Delta P_{tie12}$	0.0003	<b>-0.0041</b>	40	-	-0.0058	<b>21</b>
$\Delta P_{tie23}$	0.0041	<b>-0.0001</b>	32.23	<b>0.0011</b>	-0.001	<b>31</b>
$\Delta P_{tie13}$	0.0003	-0.0108	40.28	-	<b>-0.0056</b>	<b>17</b>

Note: Bold values indicate dominating values

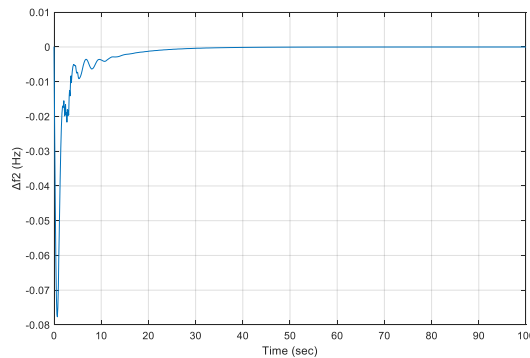
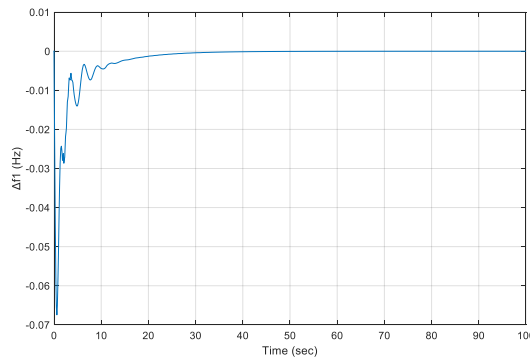
**Table (4):** Demerit index for different analysis under nominal conditions for F (Fuzzy-IDD controllers) and S (Fuzzy-SMC-PI controllers)

	$\Delta f_1$		$\Delta f_2$		$\Delta f_3$		$\Delta P_{tie12}$		$\Delta P_{tie23}$		$\Delta P_{tie13}$	
	F	S	F	S	F	S	F	S	F	S	F	S
Nominal Case	174.5	<b>170.8</b>	605.6	<b>441</b>	588	<b>400</b>	1,600	<b>441</b>	1,038	<b>961</b>	1,622	<b>289</b>
3% SLP in area-1 and area-2	1,745.6	<b>361</b>	1,518.7	<b>324</b>	1,508	<b>441</b>	1,609	<b>676</b>	<b>1,766</b>	718	3,113.6	<b>625</b>
1% SLP in all areas	1,528.8	<b>1,489.9</b>	<b>1,395</b>	1,672.8	1,310	<b>1,303</b>	1,667	<b>1,655</b>	<b>1,660</b>	2,218	2,970	<b>2,275</b>

**4.1 The System Response of Scenario 2**

Both area-1 and area-2 are provided with a 3% SLP. Fig. 7 shows the system dynamic responses of the Fuzzy-SMC-PI controller and the results are reported in Table 5. Data provided in Table 5 gives the comparative performance analysis of

both the controllers. The DI values of both controllers are presented in Table 4 (second row). The system dynamic responses and DI values comparison for this case indicates domination of Fuzzy-SMC-PI over Fuzzy-IDD controller except for the response  $\Delta P_{tie23}$ .



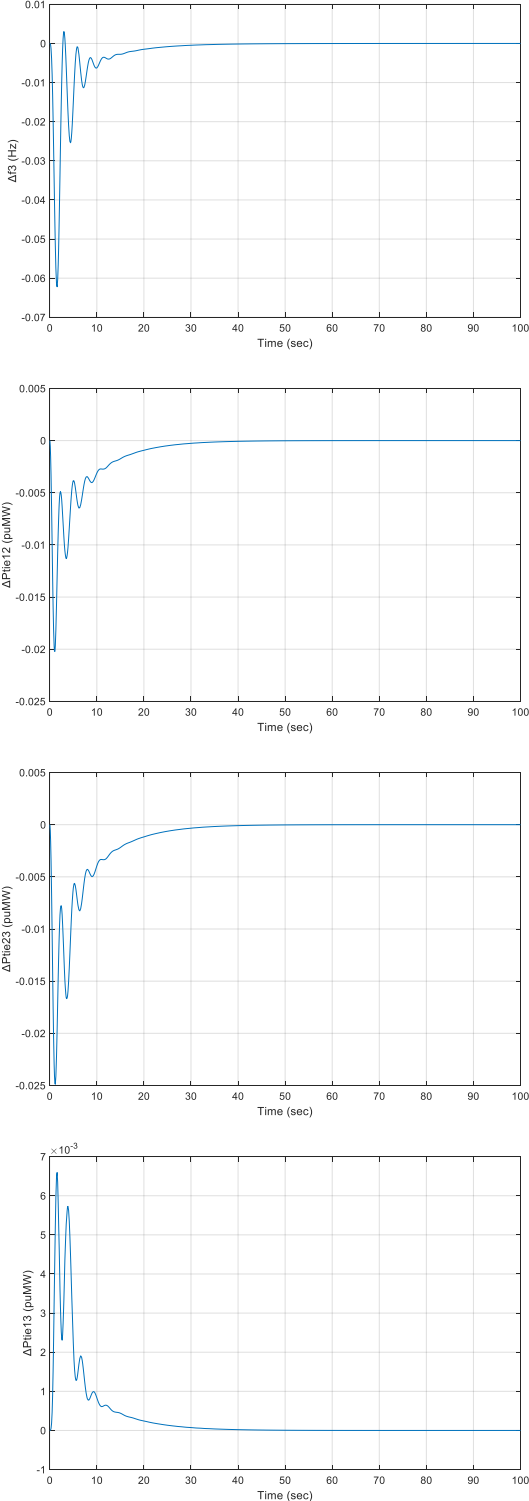


**Fig. (7):** The system response with Fuzzy-SMC-PI controller at 3% SLP in area-1 and area-2

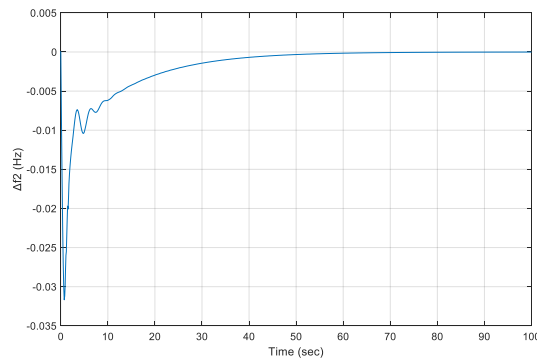
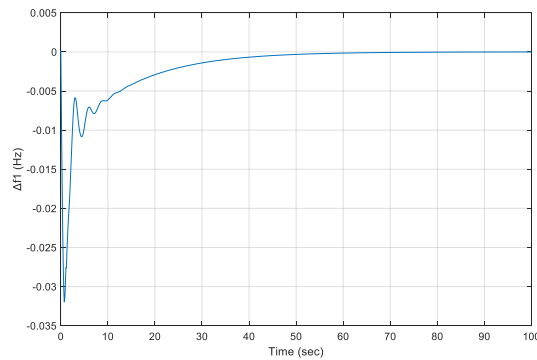
**Table (5):** The system performance for 3% SLP in area-1 and area-2

Technique	Fuzzy-IDD			Fuzzy-SMC-PI		
	MO	MU	TS	MO	MU	TS
$\Delta f_1$	0.0045	-0.1519	41.78	-	<b>-0.067</b>	<b>19</b>
$\Delta f_2$	0.0040	-0.174	38.97	-	<b>-0.077</b>	<b>18</b>
$\Delta f_3$	0.0041	-0.160	38.83	<b>0.003</b>	<b>-0.02</b>	<b>21</b>
$\Delta P_{tie12}$	0.0085	<b>-0.010</b>	40.11	-	-0.02	<b>26</b>
$\Delta P_{tie23}$	0.0172	<b>-0.0085</b>	42.02	-	-0.025	<b>26.8</b>
$\Delta P_{tie13}$	0.0203	-0.018	55.8	<b>0.0066</b>	-	<b>25</b>

**4.2 The System Response of Scenario 3**

All areas are subjected to a 1% SLP. Fig. 8 shows the system dynamic responses of the Fuzzy-SMC-PI controller and the results are reported in Table 6. Data provided in Table 6 gives the comparative performance analysis of

both the controllers. The DI values of both controllers are presented in Table 4 (third row). The system dynamic responses and DI values comparison for this case indicates domination of Fuzzy-SMC-PI over Fuzzy-IDD controller.



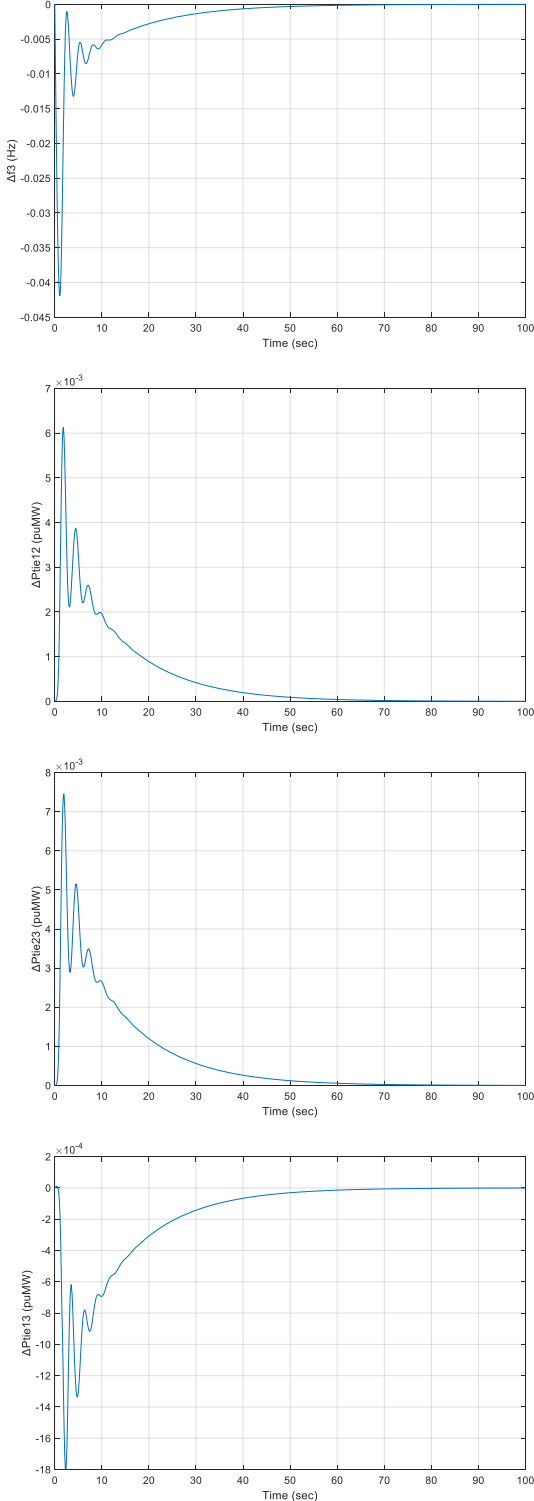


**Fig. (8):** The system response with Fuzzy-SMC-PI controllers at 1% SLP in all areas

**Table (6):** The system performance for 1% SLP in all areas

Technique	Fuzzy-IDD			Fuzzy-SMC-PI		
	MO	MU	TS	MO	MU	TS
$\Delta f_1$	0.00317	- 0.0819	39.1	-	<b>-0.031</b>	<b>38.6</b>
$\Delta f_2$	0.00319	- 0.0854	<b>37.35</b>	-	<b>-0.031</b>	40.9
$\Delta f_3$	0.00319	- 0.086	36.2	-	<b>-0.041</b>	<b>36.1</b>
$\Delta P_{tie12}$	<b>0.00085</b>	- 0.0073	40.83	0.0061	-	<b>40.69</b>
$\Delta P_{tie23}$	<b>0.00734</b>	- 0.0009	<b>40.74</b>	0.0074	-	47.1
$\Delta P_{tie13}$	0.0114	- 0.0030	54.5	-	-	<b>47.7</b> <b>0.0018</b>

## 5. CONCLUSION

This study proposes a novel Fuzzy-SMC-PI controller for LFC in modern power systems with RES. Compared to traditional methods, the Fuzzy-SMC-PI controller demonstrates significant improvements in frequency regulation performance and it effectively tackles the challenges associated with RES intermittency and variability, showcasing its adaptability to dynamic system behavior. As evidenced by a lower DI under nominal conditions and different disturbances, the controller achieves superior results with reduced overshoots, undershoots, and settling times.

1. For example, under a 1% SLP in area-1, the DI of the Fuzzy-SMC-PI controller in area-1 was 170.8, compared to 174.5 for the Fuzzy-IDD controller. Similarly, under a 3% SLP variation in area-1 and area-2, the DI of the Fuzzy-SMC-PI controller in area-2 was 324, compared to 1518.7 for the Fuzzy-IDD controller. As well as, under a 1% SLP variation in all areas, the DI of the Fuzzy-SMC-PI controller in area-3 was 1303, compared to 1310 for the Fuzzy-IDD controller.

Furthermore, it effectively tackles the challenges associated with RES intermittency and variability, showcasing its adaptability to dynamic system behavior. However, further research is necessary to address the controller's computational complexity, tuning requirements, communication delays, and model uncertainties.

Additionally, the initial application in a multi-area hybrid system with EVs suggests promise for controlling frequency and tie-line power exchange. Overall, the Fuzzy-SMC-PI controller presents a promising approach for LFC in modern power systems with RES, warranting further investigation and refinement for real-world implementation.

## 6. REFERENCES

- Aditya. (2010). Design of Load Frequency Controllers Using Genetic Algorithm for Two Area Interconnected Hydro Power System. *Electric Power Components and Systems*, 31, 81-94. doi:10.1080/15325000390112071
- Ahmad, T., Zhang, H., & Yan, B. (2020). A review on renewable energy and electricity requirement forecasting models for smart grid and buildings. *Sustainable Cities and Society*, 55, 102052. doi:<https://doi.org/10.1016/j.scs.2020.102052>
- Ali, A., Biru, G., & Banteyirga, B. (2023). Fuzzy Logic-Based AGC and AVR for Four-Area Interconnected Hydro Power System. *Electric Power Systems Research*, 224, 109494. doi:10.1016/j.epsr.2023.109494
- Anand, B., & Jeyakumar, A. E. (2008, 19-21 Nov. 2008). *Load frequency control of hydro-thermal system with fuzzy logic controller considering boiler dynamics*. Paper presented at the TENCON 2008 - 2008 IEEE Region 10 Conference.

- Aravindan, P., & Sanavullah, M. Y. (2011). *Fuzzy Logic Based Automatic Load Frequency Control of Two Area Power System With GRC*.
- Asghar, R., Riganti Fulginei, F., Wadood, H., & Saeed, S. (2023). A Review of Load Frequency Control Schemes Deployed for Wind-Integrated Power Systems. *Sustainability*, 15(10), 8380.
- Biswas, J., Bera, P., & Chakrabarty, K. (2023). Determination of control area and design of fuzzy rule-tuned PID controller for LFC of multimachine power system. *Electric Power Systems Research*, 221, 109411. doi:10.1016/j.epr.2023.109411
- Deng, Z., Xu, C., Huo, Z., Han, X., & Xue, F. (2022). Sliding Mode Based Load Frequency Control and Power Smoothing of Power Systems with Wind and BESS Penetration. *Machines*, 10(12), 1225.
- Doan, D. V., Nguyen, K., & Thai, Q. V. (2021). A Novel Fuzzy Logic Based Load Frequency Control for Multi-Area Interconnected Power Systems. *Engineering, Technology & Applied Science Research*, 11(4), 7522-7529. doi:10.48084/etasr.4320
- Farooq, Z., Rahman, A., & Lone, S. (2021). Load frequency control of multi - source electrical power system integrated with solar - thermal and electric vehicle. *International Transactions on Electrical Energy Systems*, 31. doi:10.1002/2050-7038.12918
- Gaur, P., Bhowmik, D., & Soren, N. (2019). Utilization of Plug-in Electric Vehicles for Frequency Regulation of multi-area Thermal Interconnected Power System. *IET Energy Systems Integration*, 1. doi:10.1049/iet-esi.2018.0028
- Hassan, L., Mohamed, H., Moghavvemi, M., & Yang, S. (2009). *Load Frequency Control of a Two Area Hydro Power System with Fuzzy Gain Scheduling Integral and Derivative Controller*.
- Huynh, V., Minh, B., Amaefule, E., Tran, A.-T., & Tran, P. (2021). Highly Robust Observer Sliding Mode Based Frequency Control for Multi Area Power Systems with Renewable Power Plants. *Electronics*, 10, 274. doi:10.3390/electronics10030274
- Kang, Q., Wang, L., & Wu, Q.-d. (2006). Research on Fuzzy Adaptive Optimization Strategy of Particle Swarm Algorithm.
- Khooban, M. H., & Niknam, T. (2015). A new intelligent online fuzzy tuning approach for multi-area load frequency control: Self Adaptive Modified Bat Algorithm. *International Journal of Electrical Power & Energy Systems*, 71, 254-261. doi:<https://doi.org/10.1016/j.ijepes.2015.03.017>
- Kothari, D. P. N., I.J. ; McGraw-Hill: . ( Singapore, 2003.). *Modern Power System Analysis*, 3rd ed.
- Kumar, D. M. V. (1998, 17-19 Dec. 1998). *Intelligent controllers for automatic generation control*. Paper presented at the Proceedings of IEEE TENCON '98. IEEE Region 10 International Conference on Global Connectivity in Energy, Computer, Communication and Control (Cat. No.98CH36229).
- Mi, Y., Yang, Y., Zhang, H., Yu, A., Wang, L., & Ren, L. (2014). *Sliding mode based load frequency control for multi-area interconnected power system containing renewable energy*.
- Mohamed, H., Hassan, L., Moghavvemi, M., & Yang, S. (2008). *Load frequency controller design for Iraqi National Super Grid System using fuzzy logic controller*.
- Mondai, R., & Rahman, M. M. (2017, 6-7 July 2017). *Dynamic analysis of variable structure based sliding mode intelligent load frequency control of interconnected nonlinear conventional and renewable power system*. Paper presented at the 2017 International Conference on Intelligent Computing, Instrumentation and Control Technologies (ICICICT).
- Nikzad, M., Hemmati, R., Shams, S., Farahani, A. D., Mojtaba, S., & Boroujeni, S. H. B. (2010). *Comparison of Artificial Intelligence Methods for Load Frequency Control Problem*.
- Qian, D., Tong, S., Liu, H., & Liu, X. (2016). Load frequency control by neural-network-based integral sliding mode for nonlinear power systems with wind turbines. *Neurocomputing*,

- 173, 875-885.  
doi:<https://doi.org/10.1016/j.neucom.2015.08.043>
- Rerkpreedapong, D., Hasanovic, A., & Feliachi, A. (2003). Robust load frequency control using genetic algorithm and linear matrix inequalities. *Power Systems, IEEE Transactions on*, 18, 855-861. doi:10.1109/TPWRS.2003.811005
- Sabahi, K., Sharifi, A., Aliyari-Shoorehdeli, M., M, T., & Aliasghary, M. (2008). Load Frequency Control in Interconnected Power System Using Multi-Objective PID Controller. *Journal of Applied Sciences*, 8. doi:10.1109/SMCIA.2008.5045963
- Saha, A., & Saikia, L. (2018). Renewable energy source - based multiarea AGC system with integration of EV utilizing cascade controller considering time delay. *International Transactions on Electrical Energy Systems*, 29. doi:10.1002/etep.2646
- Tasnin, W., & Saikia, L. C. (2017). Maiden application of an sine-cosine algorithm optimised FO cascade controller in automatic generation control of multi-area thermal system incorporating dish-Stirling solar and geothermal power plants. *Iet Renewable Power Generation*, 12, 585-597.
- Vrdoljak, K., Peric, N., & Petrovic, I. (2010). Sliding mode based load-frequency control in power systems. *Electric Power Systems Research*, 80, 514-527. doi:10.1016/j.epsr.2009.10.026
- Xu, Y., Ma, Y., Han, Y., Hu, T., Lun, X., & Mi, Y. (2020, 22-24 Aug. 2020). *Load Frequency Control for Renewable Energy Power System Based on Sliding Mode control with Hybrid Energy Storage*. Paper presented at the 2020 Chinese Control And Decision Conference (CCDC).
- Yang, M., Yang, Y., Han, Z., Aiqing, Y., Limin, W., & Lufei, R. (2014, 31 Aug.-3 Sept. 2014). *Sliding mode based load frequency control for multi-area interconnected power system containing renewable energy*. Paper presented at the 2014 IEEE Conference and Expo Transportation Electrification Asia-Pacific (ITEC Asia-Pacific).

#### APPENDIX A.

Nominal system parameters:  $f = 60 \text{ Hz}$ ; loading = 50%;  $K_{pi} = 120 \text{ Hz/(p.u.MW)}$ ;  $T_{pi} = 20\text{s}$ ;  
 $R_i = 2.4 \text{ Hz/p.u.MW}$ ;  $D_i = 8.33 \times 10^{-3} \text{ p.u.MW/Hz}$ ;  $Bias_i = \beta_i = 0.425 \text{ p.u.MW/Hz}$ ;  $H_i = 5 \text{ seconds}$ ;  
 $a_{12} = -2/3$ ;  $a_{23} = -3/4$ ;  $a_{13} = -1/2$ . Solar unit:  $K_{STS} = 1$ ;  $T_{STS} = 1$ ; Electric vehicle:  $N_{EV_i} = 1$ ,  $K_{EV_i} = 1$ ,  $T_{EV_i} = 1 \text{ second}$ ; Thermal unit:  $T_{ti} = 0.3 \text{ second}$ ,  $T_{gi} = 0.08 \text{ second}$ ,  $T_{ri} = 10 \text{ seconds}$ ,  $K_{ri} = 0.5$ ;  
 $GRC=0.03$ ;  $apf_{11}=0.8$ ;  $apf_{12}=0.2$ ;  $apf_{13}=0.2$ ;  
 $apf_{21}=0.8$ ;  $apf_{22}=0.2$ ;  $apf_{23}=0.2$ ;  $apf_{31}=0.7$ ;  
 $apf_{32}=0.3$ ;  $T=0.086$ ;